

# Thermal stability of azurite and malachite in relation to the formation of mediaeval glass and glazes

R.L. Frost<sup>\*</sup>, Z. Ding, J.T. Kloprogge, W.N. Martens

*Centre for Instrumental and Developmental Chemistry, Queensland University of Technology, 2 George Street,  
G.P.O. Box 2434, Brisbane, Qld. 4001, Australia*

Received 23 October 2001; received in revised form 14 February 2002; accepted 20 February 2002

## Abstract

Azurite and malachite have been extensively used as pigments in ancient and medieval manuscripts, glasses and glazes. The thermal stability of naturally occurring azurite and malachite was determined using a combination of controlled rate thermal analysis (CRTA) combined with mass spectrometry and infrared emission spectroscopy. Both azurite and malachite thermally decompose in six overlapping stages but the behavior is different for the two minerals. These stages occur around 282, 328, 350, 369, 384 and 840 °C for azurite and 250, 321, 332, 345, 362 and 842 °C for malachite. The first two stages are associated with the loss of water, whereas stages 3 and 4 result from the simultaneous loss of water and carbon dioxide. The sixth stage is associated with reduction of cupric oxide to cuprous oxide and finally to copper. Infrared emission spectroscopy shows that dehydroxylation occurs before the loss of carbonate and that the thermal decomposition is complete by 375 °C. The implication of this research is that in the preparation of glass or glazes using these two hydroxy-carbonate minerals of copper the samples will decompose at low temperatures and any color formation in the glass is not due to azurite or malachite. © 2002 Elsevier Science B.V. All rights reserved.

*Keywords:* Azurite; Malachite; Controlled rate thermal analysis; Differential thermogravimetric analysis

## 1. Introduction

Azurite ( $\text{Cu}^{2+}_3(\text{CO}_3)_2(\text{OH})_2$ ) and malachite ( $\text{Cu}^{2+}_2(\text{CO}_3)(\text{OH})_2$ ) are both monoclinic hydroxy-carbonates of copper. The kinetic behavior of the thermal decomposition of synthetic malachite was investigated by means of controlled rate thermal analysis (CRTA) under different conditions of reduced pressure, flowing gases and quasi-isobaric atmospheres [1,2]. The use of thermogravimetry (TG) to assess the effect of mechanochemical activation by dry grinding of malachite

determined the mass loss of water and carbon dioxide separately and/or together for  $\text{Cu}_2(\text{OH})_2\text{CO}_3$  samples untreated and ground for different times [3]. Often the thermal analysis is used to determine the effectiveness of catalyst precursors [4]. The thermal decomposition of basic copper carbonate (malachite,  $\text{CuCO}_3 \cdot \text{Cu}(\text{OH})_2$ ) in a dynamic atmosphere of air or nitrogen was studied via TG, differential thermogravimetric analysis (DTA) and DSC at different heating rates showed that in air  $\text{CuCO}_3 \cdot \text{Cu}(\text{OH})_2$  released  $0.5\text{H}_2\text{O}$  at 195 °C, transforming into the azurite structure  $2\text{CuCO}_3 \cdot \text{Cu}(\text{OH})_2$ . Decomposition then commenced, through two endothermic steps maximized at 325 and 430 °C [5,6]. TG and evolved gas analysis (EGA) studies of malachite,  $\text{CuCO}_3 \cdot \text{Cu}(\text{OH})_2$  and azurite,

<sup>\*</sup> Corresponding author. Tel.: +61-7-3864-2407;  
fax: +61-7-3864-1804.  
E-mail address: r.frost@qut.edu.au (R.L. Frost).

$2\text{CuCO}_3 \cdot \text{Cu}(\text{OH})_2$ , heated in He carrier gas at  $10\text{ }^\circ\text{C min}^{-1}$  show that malachite decomposition in a single step at  $380\text{ }^\circ\text{C}$ , in which  $\text{H}_2\text{O}$  and  $\text{CO}_2$  are lost simultaneously. By contrast, the two azurites studied both decompose under these conditions in two, approximately equal steps, losing one-half of their  $\text{CO}_2$  and  $\text{H}_2\text{O}$  content in each step [7].

Previous studies have determined the thermal decomposition of azurite and malachite under dynamic conditions. Azurite showed in DTA endothermic effects at  $420$  and at  $1100\text{ }^\circ\text{C}$ , malachite at  $390$  and at  $1190\text{ }^\circ\text{C}$ , and the pseudomorph of malachite after azurite at  $370$  and  $1085\text{ }^\circ\text{C}$ . At the first endothermic effect, tenorite is formed; at the second endothermic effect, reduction of  $\text{CuO}$  into  $\text{Cu}_2\text{O}$  takes place with constancy of weight being reached at  $660\text{ }^\circ\text{C}$ . It was found that the volatile ingredients,  $\text{CO}_2$  and  $\text{H}_2\text{O}$ , were released simultaneously [8]. Whereas early studies have shown that the thermal decomposition occurred at temperatures below  $200\text{ }^\circ\text{C}$  [9]. Azurite and malachite were two minerals used as coloring chemicals in ancient manuscripts, glass, tiles and ceramic materials [10–12]. However, the thermal analysis of naturally occurring azurite and malachite is very limited, particularly using modern thermo-analytical techniques. This paper reports the thermal, mass spectrometric

and infrared emission analyses of the thermal decomposition of azurite and malachite.

## 2. Experimental techniques

### 2.1. Origin of samples

The azurite was obtained from Girilambone copper mine, Girilambone, north of Nygyn, NSW. The malachite was obtained from Burra, South Australia. The samples were analyzed for phase purity by X-ray diffraction and for composition by ICP-AES. The samples were found to be phase pure and analyzed close to the theoretical composition.

### 2.2. Thermal analysis

Thermal decomposition of the basic copper carbonate minerals was carried out in a TA high-resolution thermogravimetric analyzer (series Q500) in a flowing nitrogen atmosphere ( $80\text{ cm}^3\text{ min}^{-1}$ ) at a pre-set, constant decomposition rate of  $0.15\text{ mg min}^{-1}$  (below this threshold value the samples were heated under dynamic conditions at a uniform rate of  $2.0\text{ }^\circ\text{C min}^{-1}$ ). The samples were heated in an open platinum crucible at

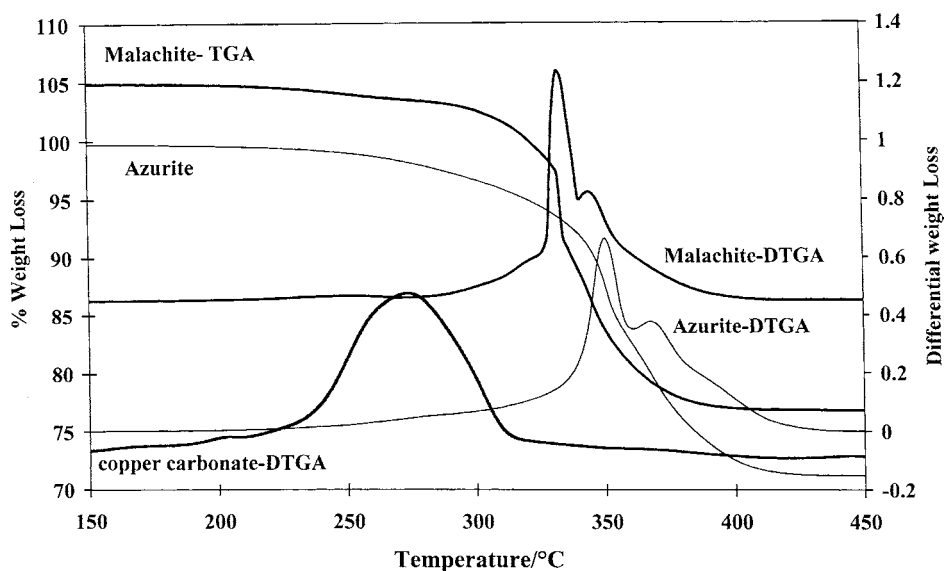


Fig. 1. Thermogravimetric and differential thermogravimetric analyses of azurite, malachite and copper carbonate.

Table 1  
The results of the stages of the thermal decomposition

	Azurite		Malachite			
	Temperature <sup>a</sup> (°C)	Theoretical weight loss (%)	Temperature <sup>a</sup> (°C)	Theoretical weight loss (%)	Proposed thermal reaction of azurite ( $\text{Cu}^{2+}_3(\text{CO}_3)_2(\text{OH})_2$ )	Proposed thermal reaction of malachite ( $\text{Cu}^{2+}_2(\text{CO}_3)(\text{OH})_2$ )
Step 1	282 (3.1)	5.2	250 (1.7)	8.1	Loss of $\text{CO}_2$ probably from some free $\text{CuCO}_3$ present	Loss of OH units as water
Step 2	328 (2.5), total dehydroxylation = 5.6%		321 (5.2)		Loss of OH units—dehydroxylation: $\text{Cu}^{2+}_3(\text{CO}_3)_2(\text{OH})_2 \rightarrow 2\text{Cu}^{2+}_3(\text{CO}_3)_2(\text{OH}) + \text{H}_2\text{O}$	Loss of OH units—dehydroxylation: $\text{Cu}^{2+}_2(\text{CO}_3)(\text{OH})_2 \rightarrow 2\text{Cu}^{2+}_2(\text{CO}_3)_2(\text{OH}) + \text{H}_2\text{O}$
Step 3	350 (10.7)	25.5	332 (9.4)	19.9	Possible $\text{Cu}^{2+}_3(\text{CO}_3)_2(\text{OH}) \rightarrow \text{CuCO}_3 \cdot \text{CuO} + \text{CO}_2 + \text{H}_2\text{O}$	$\text{Cu}^{2+}_2(\text{CO}_3)_2(\text{OH}) \rightarrow \text{CuCO}_3 + \text{CuO} + \text{CO}_2 + \text{H}_2\text{O}$
Step 4	369 (5.9)		345 (5.9)		Loss of water and carbon dioxide: $\text{Cu}^{2+}_3(\text{CO}_3)_2(\text{OH}) \rightarrow \text{CuCO}_3 + \text{CO}_2 + \text{H}_2\text{O}$	Loss of water and carbon dioxide: $\text{Cu}^{2+}_2(\text{CO}_3)_2(\text{OH}) \rightarrow \text{CuCO}_3 + \text{CO}_2 + \text{H}_2\text{O}$
Step 5	384 (6.3), total decarboxylation = 22.9		362 (6.7), total decarboxylation = 21.95		Loss of carbon dioxide only: $\text{CuCO}_3 \rightarrow \text{CuO} + \text{CO}_2$	Loss of carbon dioxide only: $\text{CuCO}_3 \rightarrow \text{CuO} + \text{CO}_2$
Step 6	840 (8.2)		842 (6.4)		Loss of oxygen: $\text{CuO} \rightarrow \text{Cu}_2\text{O} + \text{O}_2$ , $\text{Cu}_2\text{O} \rightarrow \text{Cu} + \text{O}_2$	Loss of oxygen: $\text{CuO} \rightarrow \text{Cu}_2\text{O} + \text{O}_2$ , $\text{Cu}_2\text{O} + \text{O}_2 \rightarrow \text{Cu} + \text{O}_2$

<sup>a</sup> The respective values for weight loss (% per unit area) are given in parentheses.

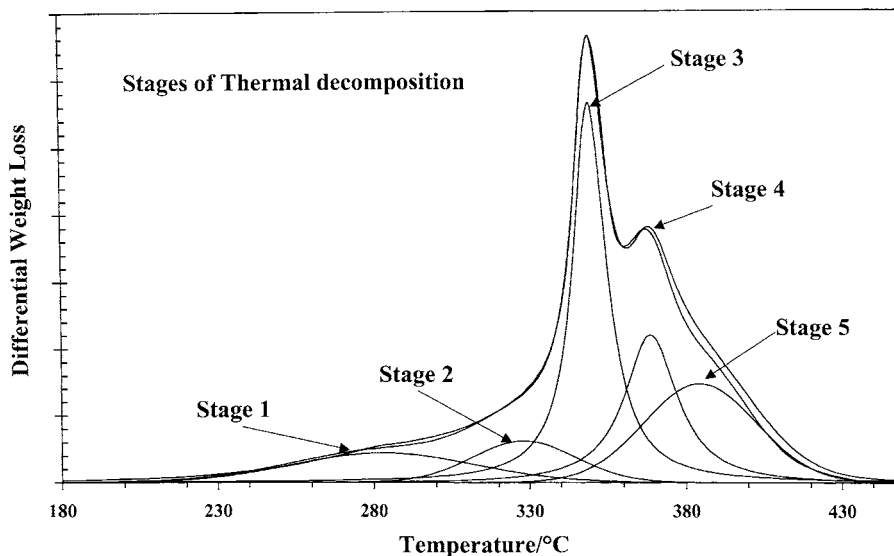


Fig. 2. Component analysis of the differential thermogravimetric analysis of azurite.

a rate of  $2.0\text{ }^{\circ}\text{C min}^{-1}$  up to  $300\text{ }^{\circ}\text{C}$ . With the quasi-isothermal, quasi-isobaric heating program of the instrument the furnace temperature was regulated precisely to provide a uniform rate of decomposition in the main decomposition stage. The TGA instrument was coupled to a Balzers (Pfeiffer) mass spectrometer for gas analysis. Selected gases only were analyzed.

### 2.3. Infrared emission spectroscopy

FT-IR emission spectroscopy was carried out on a Nicolet spectrometer equipped with a TGS detector, which was modified by replacing the IR source with an emission cell. A description of the cell and principles of the emission experiment have been published

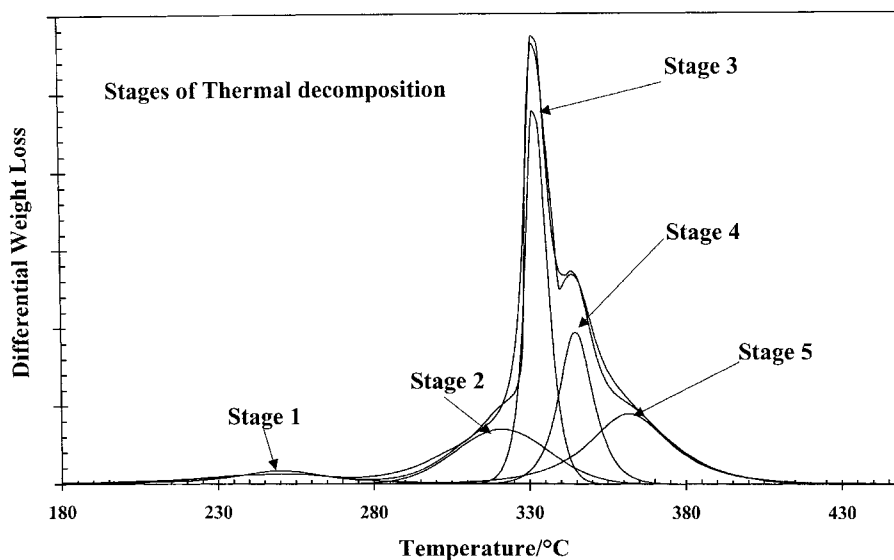


Fig. 3. Component analysis of the differential thermogravimetric analysis of malachite.

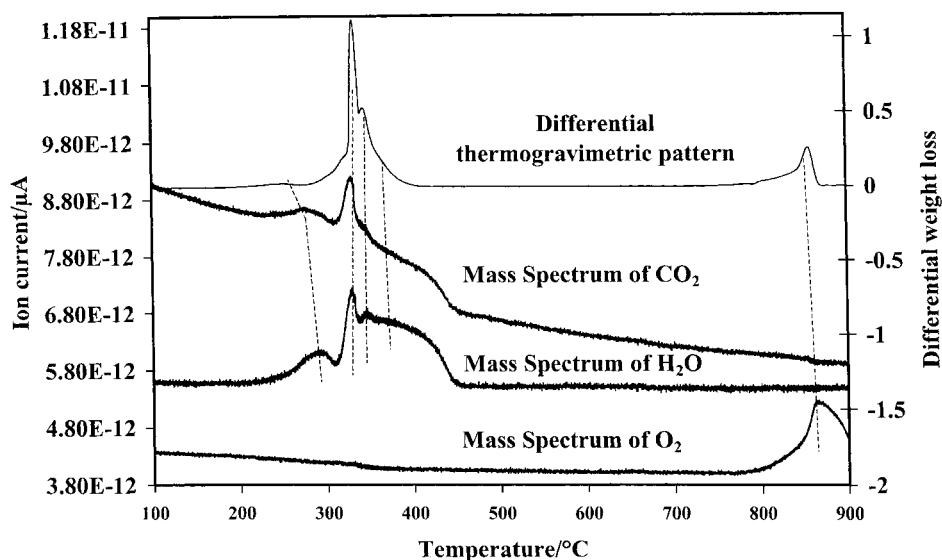


Fig. 4. Mass spectrum of water, carbon dioxide and oxygen and the differential thermogravimetric pattern of malachite.

elsewhere [13–17]. Approximately 0.2 mg of the basic copper carbonate mineral was spread as a thin layer (approximately 0.2  $\mu\text{m}$ ) on a 6 mm diameter platinum surface and held in an inert atmosphere within a nitrogen-purged cell during heating.

In the normal course of events, three sets of spectra are obtained: firstly the black body radiation over the

temperature range selected at the various temperatures, secondly the platinum plate radiation is obtained at the same temperatures and thirdly the spectra from the platinum plate covered with the sample. Normally only one set of black body and platinum radiation is required. The emittance spectrum ( $E$ ) at a particular temperature was calculated by subtraction of the

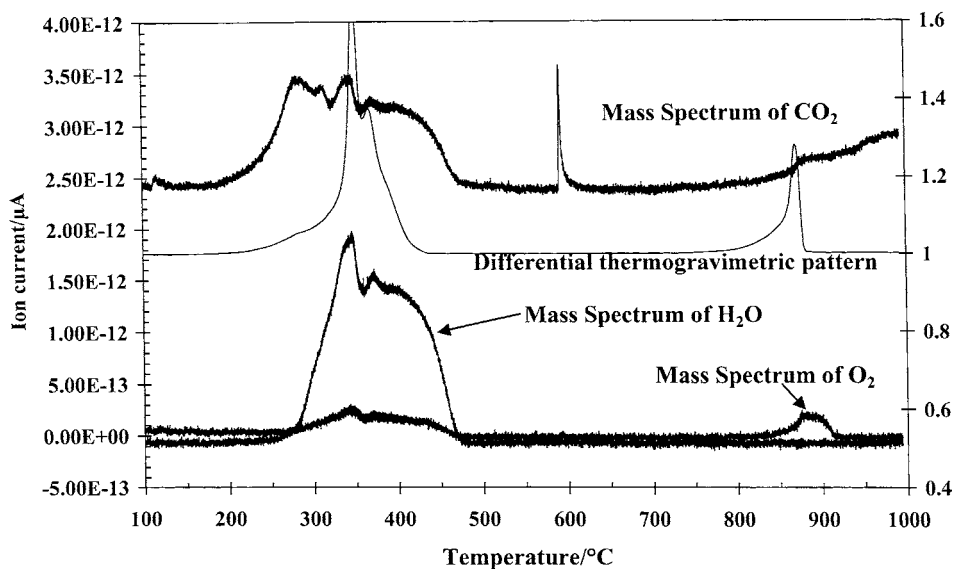


Fig. 5. Mass spectrum of water, carbon dioxide and oxygen and the differential thermogravimetric pattern of azurite.

single beam spectrum of the platinum backplate from that of the platinum + sample, and the result ratioed to the single beam spectrum of an approximate black-body (graphite). The following equation was used to calculate the emission spectra:

$$E = -0.5 \log \frac{\text{Pt} - \text{S}}{\text{Pt} - \text{C}}$$

This spectral manipulation is carried out after all the spectral data has been collected. The emission spectra were collected at intervals of 50 °C over the range 200–750 °C. The time between scans (while the temperature was raised to the next hold point) was, approximately 100 s. It was considered that this was sufficient time for the heating block and the powdered sample to reach temperature equilibrium. The spectra were acquired by

coaddition of 64 scans for the whole temperature range (approximate scanning time 45 s), with a nominal resolution of 4 cm<sup>-1</sup>. Good quality spectra can be obtained providing the sample thickness is not too large. If too large a sample is used then the spectra become difficult to interpret because of the presence of combination and overtone bands. Spectral manipulation such as baseline adjustment, smoothing and normalization was performed using the GRAMS<sup>®</sup> software package (Galactic Industries Corporation, Salem, NH, USA).

### 3. Results and discussion

Previous studies of the thermal decomposition of malachite are varied and the results depend upon the

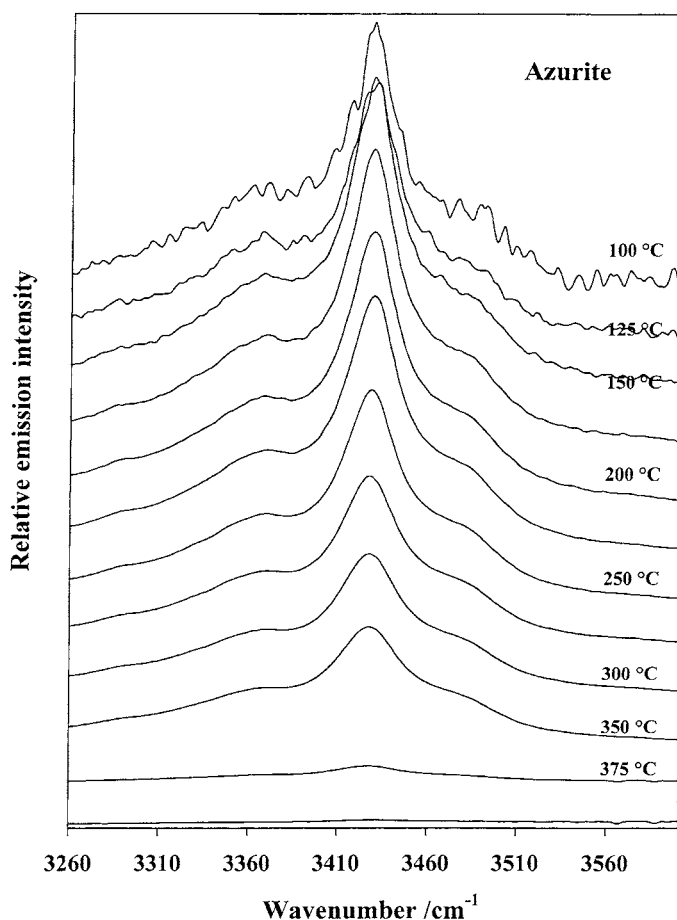


Fig. 6. Infrared emission spectra of the hydroxyl-stretching vibrations of azurite.

way the experiments are undertaken. Wide variation in the interpretation of the results for naturally occurring malachite is reported [7–9]. Fig. 1 shows the thermal decomposition of azurite and malachite, respectively. The figure also shows the thermal decomposition of copper carbonate for comparison. The results of the stages of the thermal decomposition are shown in Table 1. Six stages of decomposition are identified: (a) firstly in the 180–430 °C region and (b) in the ~840 °C region. The first five stages for the low temperature decomposition are illustrated in Figs. 2 and 3. These figures show the peak component analysis of the differential weight loss of azurite and

malachite, respectively. The theoretical weight loss of azurite based upon the formula  $\text{Cu}^{2+}_3(\text{CO}_3)_2(\text{OH})_2$  is 5.2% for the OH units and 25.5% for the  $\text{CO}_2$ , making a total of 30.7%. The theoretical weight loss for malachite based upon the formula  $\text{Cu}^{2+}_2(\text{CO}_3)(\text{OH})_2$  is 8.1% for the OH units and 19.9% for the  $\text{CO}_2$ , making a total of 28%. The measured weight losses for azurite and malachite are 28.5 and 28.9%, respectively. Thus, the measured weight loss for malachite is very close to the theoretical value and the weight loss for azurite is less than the predicted value. In the case of malachite the small difference might be accounted for by adsorbed water. An additional weight

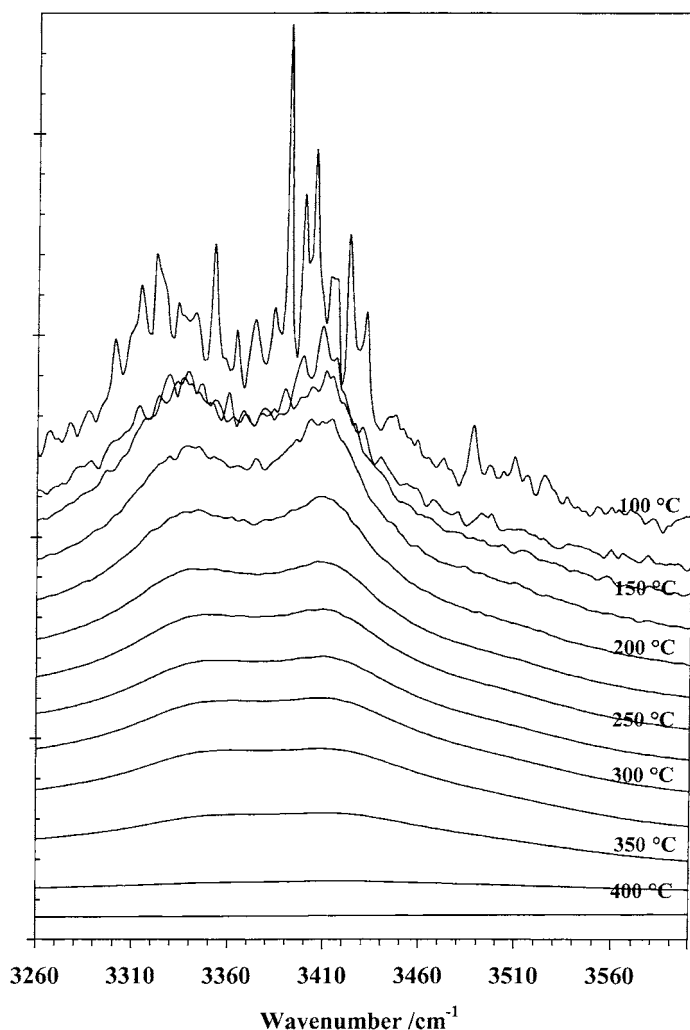


Fig. 7. Infrared emission spectra of the hydroxyl-stretching vibrations of malachite.

loss step is observed at 840 °C and the weight loss was 8.2% for malachite and 6.4% for azurite.

Six weight loss steps are observed for azurite and malachite. The first weight loss step for malachite is 1.7% of the total weight loss and is attributed to the loss of hydroxyl units. Figs. 4 and 5 display the mass spectrometric analyses of the evolved gases for azurite and malachite. Mass spectrometry shows that water is the only evolved gas at this step for malachite and azurite. Some dehydroxylation is occurring at this stage. Comparison of the DTGA of copper carbonate and that of azurite is noteworthy. The first weight loss step for azurite corresponds with that of copper carbonate. No copper carbonate was detected by X-ray diffraction. Step 2 is primarily a dehydroxylation step. One possible type of mechanism is displayed

in Table 1. Mass spectrometry of both azurite and malachite shows that water vapor is the evolved gas for this step and that water vapor continues to be evolved in later steps. This means the product of the decomposition must contain both carbonate and hydroxyl units. The product of this step might be  $\text{Cu}^{2+}_3(\text{CO}_3)_2(\text{OH})$  for azurite and  $\text{Cu}^{2+}_2(\text{CO}_3)_2(\text{OH})$  for malachite. The total weight loss for steps 1 and 2 for malachite is 6.9% which compared with the theoretical value of 8.1% means that 1.2% of the total OH units is lost in later steps.

The temperature in step 3 is 350 °C for azurite and 332 °C for malachite. In this step both dehydroxylation and decarboxylation is occurring. Mass spectrometry shows that both carbon dioxide and water vapor are the evolved gases for this step. The weight loss for

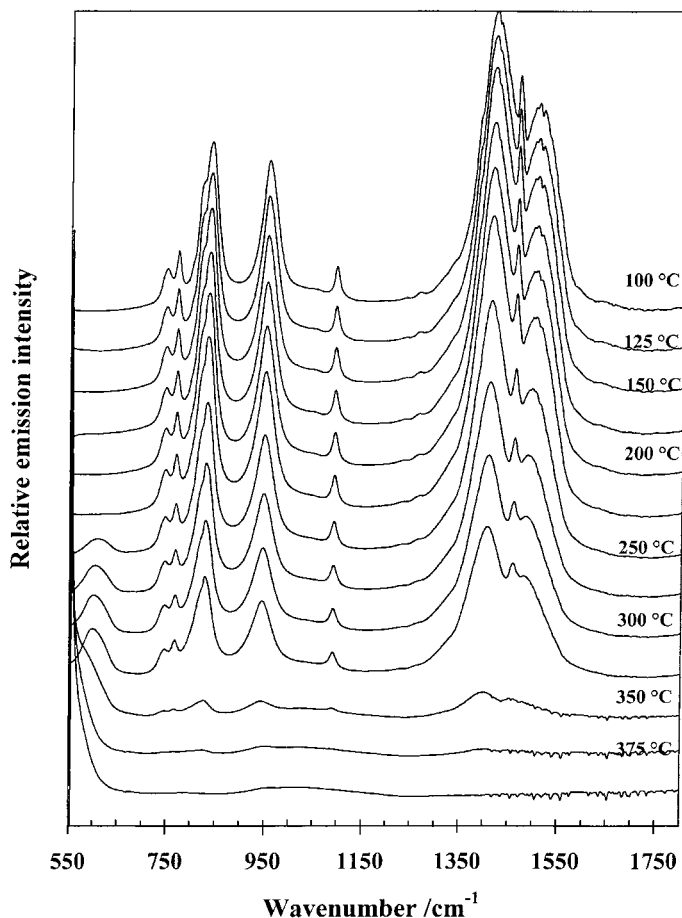


Fig. 8. Infrared emission spectra of the 550–1800  $\text{cm}^{-1}$  region of azurite.



this step is 10.7% for azurite and 9.4% for malachite. Step 5 is similar to step 4 in that both hydroxyl units and carbon dioxide are lost in the thermal transformation. It is suggested that the product of this reaction is copper oxide. Step 6 is the step where deoxygenation of the copper oxide occurs. Mass spectrometry of the evolved oxygen gas shows that the reaction occurs in two steps as is shown in Table 1. The thermal decomposition patterns of azurite and malachite are similar but not the same. However, differences in the temperature of the decomposition may be observed. Mass spectrometry shows that dehydroxylation commences at around 250 °C and is completed simultaneously with the loss of carbon dioxide at 450 °C.

Stage 3 is observed at 350 °C for azurite and at 332 °C for malachite. A weight loss of 37.6% is observed for azurite and 32.5% for malachite. For this decomposition stage, the loss of water and carbon dioxide for azurite is simultaneous and follows the same pattern. This is observed around 348 °C in the spectrometric analysis. In contrast, although the DTGA pattern shows a single step at 332 °C for malachite, the mass spectrometric analysis shows two closely overlapping steps occurring at 355 and 388 °C. Water and carbon dioxide are lost simultaneously for malachite for this stage. Stage 4 is readily observed as a separate step for both azurite and malachite at 369 and 345 °C. This stage is observed at the 7300 and 7200 cycle for

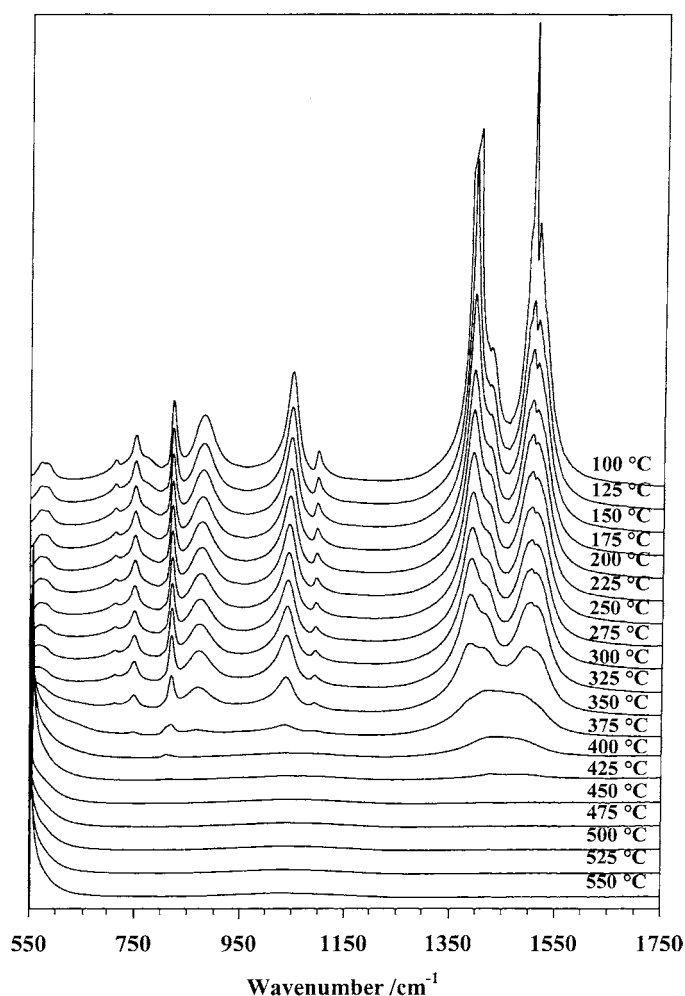


Fig. 9. Infrared emission spectra of the 550–1800 cm<sup>-1</sup> region of malachite.

azurite and malachite, respectively. The water and carbon dioxide are lost simultaneously for both azurite and malachite. Although the water and carbon dioxide are being lost together, mass spectrometry shows a loss of both water and carbon dioxide at 432 °C and this mass loss is in harmony with stage 5.

A sixth stage in the thermal decomposition of natural azurite and malachite is observed at ~840 °C. This

weight loss is associated with a loss of oxygen with no other evolved gases being observed. This weight loss is associated with the conversion of copper oxide to cuprous oxide and to copper. Such decompositions have previously been reported at ~660 °C [8]. In the dynamic experiment thermal decomposition was reported as single step at 420 °C for azurite and at 370 °C for malachite [8]. A similar conclusion was

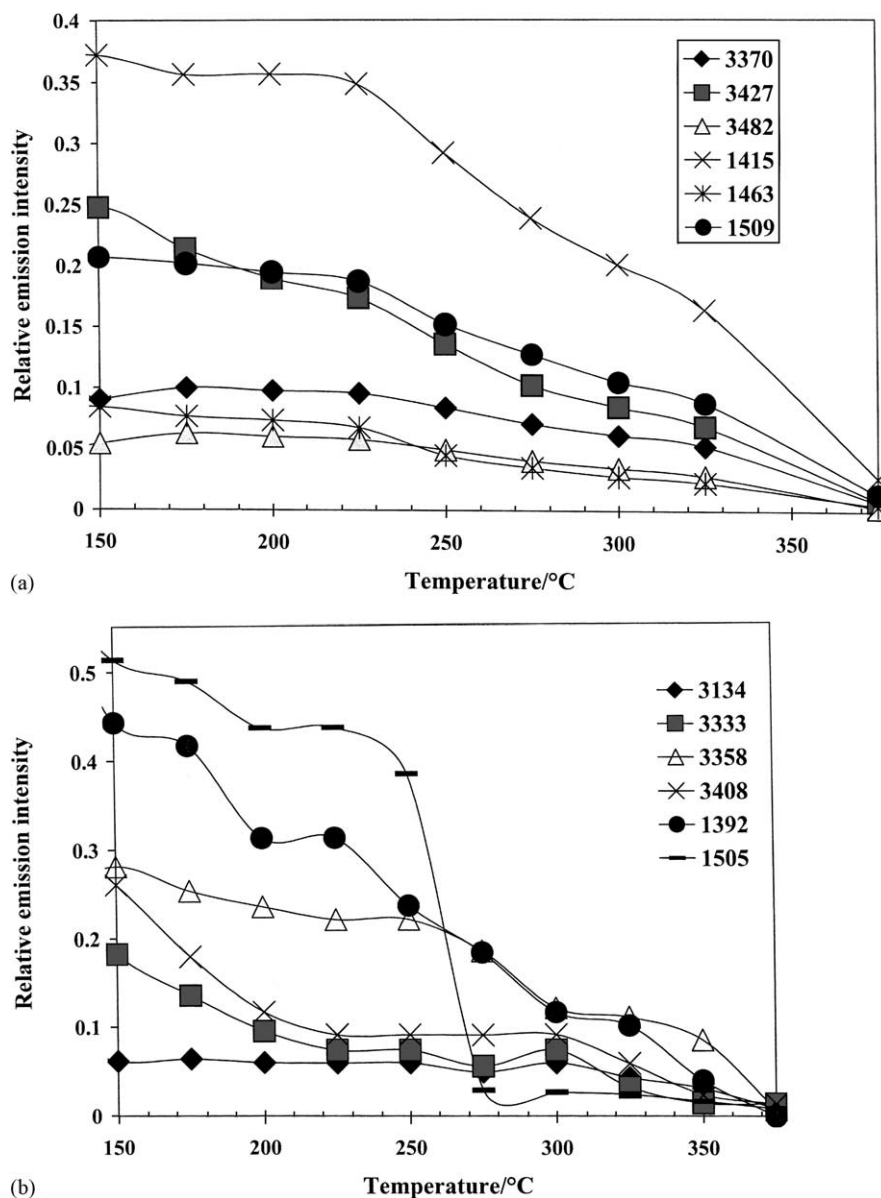


Fig. 10. Variation of band intensity as a function of temperature.

reported by others for malachite but azurite was shown to have two steps for the thermal decomposition [7]. Mansour proposed a scheme for the thermal decomposition of azurite in which an initial loss of water occurred with a conversion of the azurite to malachite followed by a simultaneous loss of water and carbon dioxide [5]. Such conclusions are in harmony with the results observed in this work. However five steps are observed for the thermal decomposition as opposed to the two steps at 320 and 430 °C reported previously [5]. Mansour reported the continuous loss of water and carbon dioxide up to 700 °C. In this work, the loss is complete by 430 °C for azurite and 400 °C for malachite.

### 3.1. Infrared emission spectroscopy of azurite and malachite

The infrared emission spectra of the hydroxyl-stretching region of azurite and malachite are shown in Figs. 6 and 7. Three hydroxyl-stretching vibrations in the infrared emission spectra of azurite are identified at 3484, 3426 and 3360  $\text{cm}^{-1}$ . The most intense band is the band at 3426  $\text{cm}^{-1}$ , which corresponds to the Raman band observed at 3420  $\text{cm}^{-1}$ . The intensity of these bands is constant up to 275 °C after which the intensity decreases until at 375 °C no intensity remains. The hydroxyls are lost in a continuous manner over this temperature range. Four hydroxyl-stretching vibrations are observed in the infrared emission spectra of malachite at 3408, 3358, 3333 and 3134  $\text{cm}^{-1}$ . Figs. 8 and 9 display the carbonate vibrations for azurite and malachite. The intensity of the carbonate remains constant up to 300 °C, and then decomposition occurs. A new infrared band is observed at 600  $\text{cm}^{-1}$ . The appearance of this band shows the temperature for the onset of thermal decomposition. Fig. 10 shows the loss of intensity of selected hydroxyl and carbonate bands for azurite and malachite. The figures clearly demonstrate that differences exist between the dehydroxylation and loss of carbon dioxide of the two minerals. The intensity of the hydroxyl bands at 3370, 3427 and 3482  $\text{cm}^{-1}$  for azurite decreases continuously from 225 °C. The intensity of the carbonate bands at 1509, 1463 and 1415  $\text{cm}^{-1}$  starts to decrease at a slightly higher temperature. This observation is in harmony with the results of the mass spectrometric analysis where

dehydroxylation commences before the loss of carbon dioxide. For malachite the intensity of the IES bands at 3134, 3333, 3358 and 3408  $\text{cm}^{-1}$  decreases over the temperature range 150–375 °C at which point no intensity remains in the bands. The intensity of the 1505  $\text{cm}^{-1}$  band shows a significant decrease in intensity at 275 °C whereas the 1392  $\text{cm}^{-1}$  band decreases constantly with temperature increase. The significant change in intensity at 275 °C of the 1505  $\text{cm}^{-1}$  band shows a phase change in the mineral is occurring at this temperature. This change is associated with the dehydroxylation. The intensity of the 1505  $\text{cm}^{-1}$  band is replaced with an increase in intensity of a band at 1425  $\text{cm}^{-1}$ . The infrared emission spectroscopy also shows that the loss of hydroxyls and the carbon dioxide occurs simultaneously.

## 4. Conclusions

A number of conclusions are drawn as follows:

- (a) The thermal decomposition of azurite and malachite are similar but not the same.
- (b) This decomposition is complex with five overlapping thermal decomposition steps identified and a sixth at elevated temperatures.
- (c) Stages 1 and 2 result from the loss of water.
- (d) Stages 3 and 4 result from the simultaneous loss of water and carbon dioxide.
- (e) The stages identified in the mass spectrometric analyses are in harmony with the steps identified in the differential thermogravimetric patterns.
- (f) Infrared emission spectroscopy showed that the hydroxyls were lost before the evolution of carbon dioxide.
- (g) Above 325 °C, both the hydroxyls and carbon dioxide are lost concurrently
- (h) IES shows that the dehydroxylation is complete by 375 °C.

Implications for the use of malachite and azurite from archaeological and mediaeval glasses and glazes rest with the decomposition of these two coloring agents at low temperatures. In any glass or glaze formation these minerals will have decomposed. An alternative methodology depends upon the coating of a surface with azurite or malachite and then placing the clear glass or glaze over this coating.

## Acknowledgements

The Centre for Instrumental and Developmental Chemistry of the Queensland University of Technology is gratefully acknowledged for financial, and infra-structural support for this project. The Australian Research Council (ARC) is thanked for the funding of the Integrated Thermal Analysis Facility.

## References

- [1] N. Koga, J.M. Criado, H. Tanaka, *Thermochim. Acta* 340/341 (1999) 387.
- [2] N. Koga, J.M. Criado, H. Tanaka, *J. Therm. Anal. Calorimetr.* 60 (2000) 943.
- [3] K. Wieczorek-Ciurowa, J.G. Shirokov, M. Parylo, *J. Therm. Anal. Calorimetr.* 60 (2000) 59.
- [4] R.H. Hoepfener, E.B.M. Doesburg, J.J.F. Scholten, *Appl. Catal.* 25 (1986) 109.
- [5] S.A.A. Mansour, *J. Therm. Anal.* 42 (1994) 1251.
- [6] H. Tanaka, M. Yamane, *J. Therm. Anal.* 38 (1992) 627.
- [7] I.W.M. Brown, K.J.D. Mackenzie, G.J. Gainsford, *Thermochim. Acta* 75 (1984) 23.
- [8] W. Kleber, *Krist. Tech.* 2 (1967) 5.
- [9] D.R. Simpson, R. Fisher, K. Libsch, *Am. Mineral.* 49 (1964) 1111.
- [10] R.J.H. Clark, *J. Mol. Struct.* 480/481 (1999) 15.
- [11] H.G.M. Edwards, D.W. Farwell, F.R. Perez, S.J. Villar, *Appl. Spectrosc.* 53 (1999) 1436.
- [12] H.G.M. Edwards, D.W. Farwell, F.R. Perez, J.M. Garcia, *Analyst* 126 (2001) 383.
- [13] R.L. Frost, A.M. Vassallo, *Clays Clay Mineral.* 44 (1996) 635.
- [14] R.L. Frost, J.T. Kloprogge, S.C. Russell, J. Szetu, *Appl. Spectrosc.* 53 (1999) 829.
- [15] J.T. Kloprogge, R.L. Frost, *Appl. Clay Sci.* 15 (1999) 431.
- [16] J.T. Kloprogge, R.L. Frost, J. Kristof, *Can. J. Anal. Sci. Spectrosc.* 44 (1999) 33.
- [17] J.T. Kloprogge, R.L. Frost, *Neues Jahrb. Mineral., Monatsh.* (2000) 145.